

Cu(InAl)Se₂ THIN FILMS AND DEVICES DEPOSITED BY MULTISOURCE EVAPORATION

M.W. Haimbodi, E. Gourmelon, P. D. Paulson, R.W. Birkmire and W.N. Shafarman
Institute of Energy Conversion, University of Delaware, Newark, Delaware USA 19716

ABSTRACT

Cu(InAl)Se₂ is investigated as an alternative high bandgap alloy of CuInSe₂ for achieving devices and modules with greater performance as bandgap and V_{OC} increase. Device efficiencies with Cu(InGa)Se₂ and CuIn(SeS)₂ decrease for bandgap greater than 1.3 eV. In this work, Cu(InAl)Se₂ thin films were deposited by four-source elemental evaporation with a composition range of 0 ≤ Al/(In+Al) ≤ 0.65 corresponding to a bandgap range 1.0 ≤ E_g ≤ 1.8 eV. All films are single phase as determined by X-ray diffraction. Characterization of optical and structural properties of the films shows that the effect of increasing Al content on bandgap and lattice spacing agrees with the results on Cu(InAl)Se₂ crystals and with calculated values. Solar cells with structure glass/Mo/Cu(InAl)Se₂/CdS/ZnO were fabricated. The best cells have 11% efficiency and V_{OC} increases with increasing Al content to greater than 0.7 V.

INTRODUCTION

Significant effort has been made in recent years by a number of research groups to develop high efficiency solar cells based on high band gap alloys of CuInSe₂. This is driven by the expectation that higher bandgap alloys will yield higher module efficiencies due to reduced losses related to series resistance, interconnects, and TCO's due to lower cell current. In addition, a high bandgap device could be used as the top cell in a tandem or multijunction cell structure. Most research on such high bandgap materials has focused on Cu(InGa)Se₂ and CuIn(SeS)₂. In all cases the highest efficiencies have been achieved with a band gap, E_g < 1.3 eV [1,2,3].

Cu(InAl)Se₂ may be a viable alternative for higher band gap CuInSe₂ based solar cells because it requires smaller relative alloy concentration than the Ga or S alloys to achieve comparable bandgap. The calculated bandgaps of the Cu(InGa)Se₂, CuIn(SeS)₂, and Cu(InAl)Se₂ alloy systems [4] are plotted in Figure 1. This shows, for example, that a Cu(InAl)Se₂ film with E_g = 1.4 eV will contain Al/(In+Al) = 0.30 while a comparable band gap Cu(InGa)Se₂ film will contain Ga/(In+Ga) = 0.65, and that of CuIn(SeS)₂ will contain S/(S+Se) = 0.77.

Previous work on Cu(InAl)Se₂ alloys has focused primarily on crystal samples [5,6,7]. Characterization of

these crystals has included optical properties and phase and structural analysis by x-ray diffraction (XRD). Thin films of Cu(InAl)Se₂ deposited by reaction of stacked layers were reported and also characterized by XRD and optical spectroscopy [8]. No Cu(InAl)Se₂ device results have been reported.

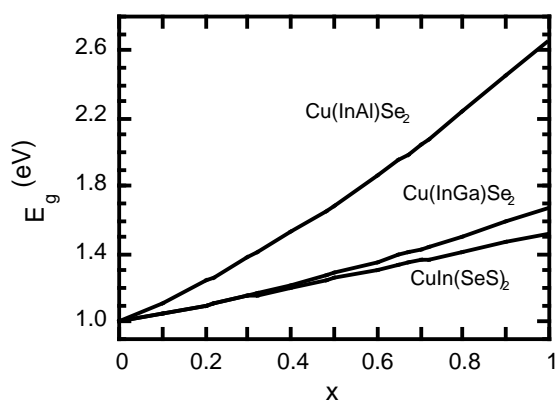


Fig. 1. Band gap of Cu(InAl)Se₂, Cu(InGa)Se₂ and CuIn(SeS)₂ alloys with x = Al/(In+Al), Ga/(In+Ga) or S/(S+Se), respectively, from Ref. [9].

This paper describes the deposition of single phase Cu(InAl)Se₂ thin films by multisource elemental evaporation. Structural and optical characterization of these films is presented and compared to results of Cu(InAl)Se₂ crystals. Solar cell results are also presented with an 11% device efficiency demonstrated.

EXPERIMENTAL DESCRIPTION

Cu(InAl)Se₂ films were deposited by multisource evaporation from elemental Cu, In, Al, and Se sources which provide coincident fluxes onto soda lime glass or Mo-coated soda lime glass substrates. Similar to processes used to deposit Cu(InGa)Se₂ described elsewhere [1], the fluxes are independently controlled via the source temperatures. All films were deposited with constant elemental fluxes throughout the deposition so there was not intentional grading of the composition. The films were deposited at substrate temperature (T_{SS})

between 450-500°C since films deposited at higher temperature did not adhere well and flaked off at the Cu(InAl)Se₂/Mo or Cu(InAl)Se₂/glass interface. All films are 1.5 - 2 μm thick.

The Cu(InAl)Se₂ films are characterized by XRD, optical transmission and reflection, and energy dispersive spectroscopy (EDS). The determination of composition by EDS for Cu(InAl)Se₂ requires the use of the Se-K line because separation between the Se-L and Al-K lines is less than the instrumental resolution of the Si(Li) detector used in the measurements. The Cu/(In+Al) ratio of the films ranges from 0.7 to 1.0 and Al/(In+Al) was varied from 0 to 0.65.

Solar cells were fabricated using the baseline processes developed for Cu(InGa)Se₂ devices [1], with structure glass/Mo/Cu(InAl)Se₂/CdS/ZnO:Al/Ni-Al grid and total cell area of 0.5 cm² defined by mechanical scribing. The devices were characterized by current-voltage (J-V) measurements under 100 mW/cm² illumination at 25 °C, and by quantum efficiency (QE) measurements under white light bias.

RESULTS: FILM CHARACTERIZATION

The compositions, determined by EDS, of the Cu(InAl)Se₂ films characterized in this paper are listed in Table 1. This includes samples deposited on bare glass and used for optical characterization and on Mo-coated glass used for XRD analysis and device fabrication. Oxygen is detected in films with high relative Al content, $x = \text{Al}/(\text{In}+\text{Al}) > 0.6$. This may result from reaction with air after deposition rather than O incorporation during deposition.

Table 1. Composition, Measured by EDS, for Cu(InAl)Se₂ Films.

| Cu (%) | In (%) | Al (%) | Se (%) | O (%) | Al/(In+Al) |
|------------------------------|--------|--------|--------|-------|------------|
| Films on glass substrates | | | | | |
| 22.2 | 25.2 | – | 52.6 | <1 | 0.00 |
| 21.1 | 22.2 | 8.0 | 48.7 | <1 | 0.26 |
| 23.1 | 18.5 | 10.0 | 48.4 | <1 | 0.35 |
| 21.5 | 16.1 | 15.0 | 47.4 | <1 | 0.48 |
| 23.0 | 9.1 | 16.9 | 46.2 | 4.8 | 0.65 |
| Films on glass/Mo substrates | | | | | |
| 24.5 | 25.6 | – | 49.9 | <1 | 0.00 |
| 23.4 | 22.1 | 7.9 | 46.6 | <1 | 0.26 |
| 21.8 | 19.9 | 11.7 | 46.6 | <1 | 0.37 |
| 22.2 | 14.6 | 16.3 | 46.9 | <1 | 0.53 |

The Cu(InAl)Se₂ films are all found to be single phase within the detection limits of XRD analysis. The XRD spectrum of a film with Al/(In+Al) = 0.63, and Cu/(In+Al) = 0.8 is shown in Fig. 2. All peaks shown correspond to either Cu(InAl)Se₂ or Mo. The Cu(InAl)Se₂ peaks shift to higher 2θ as the Al content increases due to a decrease in d-spacing. The normalized (112) reflections are shown in Fig. 3 for four films with Al/(Al + In) = 0.0, 0.26, 0.36 and 0.53. There is considerable broadening observed in the XRD peaks of some samples, such as the sample with $x =$

0.53 in Fig. 3. This could be due to stress in the films, which could also be the cause for poor adhesion, or a compositional distribution in the Cu(InAl)Se₂ film.

The lattice spacing d(112) was determined from the peak positions of each sample in Fig. 3, using the Mo reflection as an internal standard in each case. The d(112) spacings are shown in Fig. 4 along with d(112) for crystal samples calculated from the lattice parameters in ref [5]. Also shown is the linear fit to the JCPDS values for CuInSe₂ (JCPDS #40-1487) and CuAlSe₂ (JCPDS #44-1269) [9] which assumes that the lattice spacing follows Vegard's law for the Cu(InAl)Se₂ system. The results demonstrate that the Cu(InAl)Se₂ films and the crystals fit this linear relation.

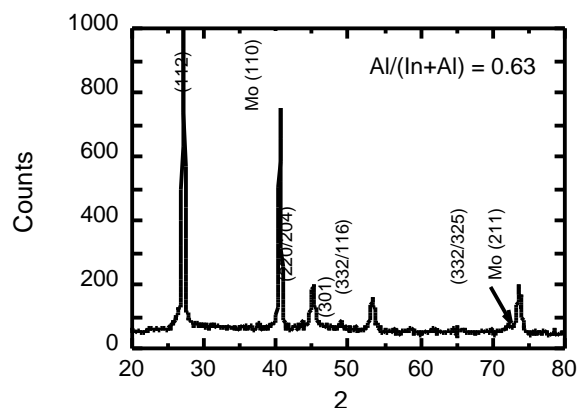


Fig. 2. X-ray diffraction spectrum of a Cu(InAl)Se₂/Mo sample with Al/(In+Al) = 0.63, and Cu/(In+Al) = 0.8., showing single phase Cu(InAl)Se₂.

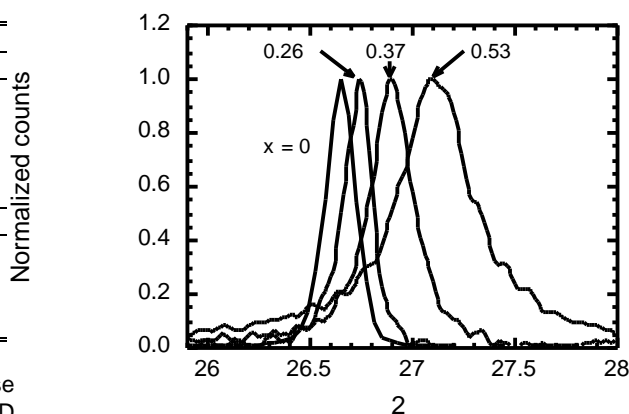


Fig. 3. XRD spectra of the (112) reflection for films with increasing Al content.

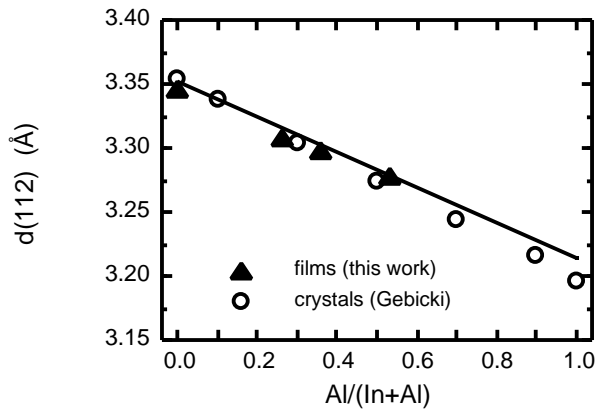


Fig. 4. Lattice spacing $d(112)$ for samples with increasing Al content, showing fit to Vegard's law.

The normalized optical transmission, $T/(1-R)$, for four $\text{Cu}(\text{InAl})\text{Se}_2$ films and a CuInSe_2 sample are shown in Fig. 5. The transmission for all films approaches 90-100% for $E < E_g$, which is necessary for use in a tandem cell. The optical bandgaps were determined from the intercepts of $(E - E_g)^2$ vs. E , as indicated in Fig. 6. The increase in the bandgap with increasing Al content agrees well with calculated fit to [4]:

$$E_g(x) = (1-x)E_g(A) + xE_g(B) - bx(1-x) \quad (1)$$

where $E_g(A) = 1.0$ eV for CuInSe_2 , $E_g(B) = 2.7$ eV for CuAlSe_2 , and the optical bowing parameter, $b = 0.59$, for $\text{Cu}(\text{InAl})\text{Se}_2$. Also shown in Fig. 7 is the crystal data from references [5] and [6].

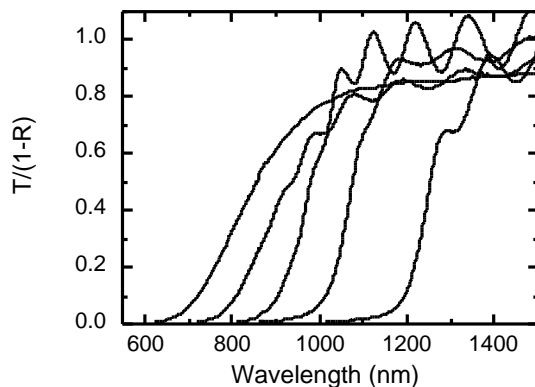


Fig. 5. Normalized optical transmission, $T/(1-R)$, for $\text{Cu}(\text{InAl})\text{Se}_2$ films with $x = 0, 0.26, 0.35, 0.48,$ and 0.65 , from right to left.

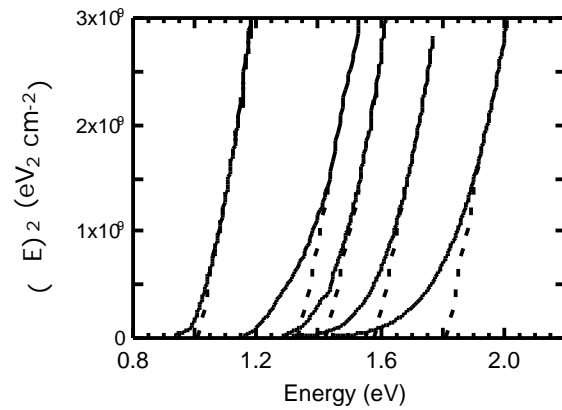


Fig. 6. Bandgap determination for $\text{Cu}(\text{InAl})\text{Se}_2$ films.

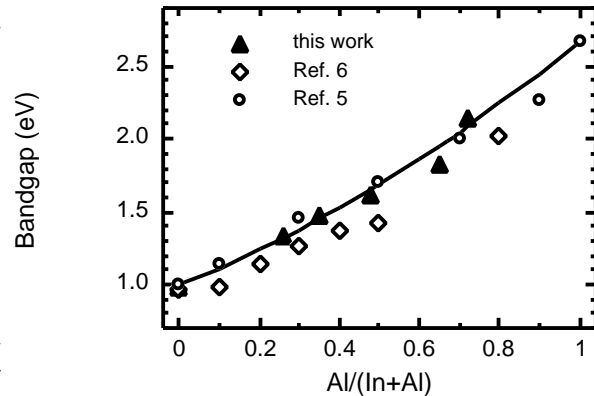


Fig. 7. Optical bandgap of $\text{Cu}(\text{InAl})\text{Se}_2$ thin films compared to crystal results. The line is the curve from Eq. 1.

RESULTS: DEVICES

Solar cells have been fabricated and the J-V parameters for the best cells with $x = 0.26, 0.37,$ and 0.53 are listed in Table 2, where E_g is determined from x using Eq. 1. The J-V curves, under $100\text{mW}/\text{cm}^2$ illumination and in the dark, are shown in Fig. 8 for these devices. A CuInSe_2 cell, shown for comparison, had the CuInSe_2 layer deposited in the same system under comparable conditions including $T_{\text{SS}} = 450^\circ\text{C}$. The results listed were measured after the devices were annealed in air for 2-5 minutes at 200°C , which typically resulted in a 20-50 mV increase in V_{OC} and little other change. The best devices have $\sim 11\%$ efficiency. V_{OC} increases with increasing band gap, but remains lower than $\text{Cu}(\text{InGa})\text{Se}_2$ devices with comparable band gap [1]. For example, a $\text{Cu}(\text{InGa})\text{Se}_2$ device with $E_g = 1.3$ eV gave $V_{\text{OC}} = 0.73\text{V}$.

Quantum efficiency curves for these devices are shown in Fig. 9. The overall collection and steepness of the long wavelength edge is comparable for the $\text{Cu}(\text{InAl})\text{Se}_2$ cells with $x = 0.26$ and 0.36 and the CuInSe_2 cell. However, there is an apparent discrepancy between the long wavelength edge of the QE curves and the band

gaps obtained from the EDS compositions. The shift in the QE edge from the CuInSe_2 is approximately 0.1, 0.25, and 0.45 eV for the $\text{Cu}(\text{InAl})\text{Se}_2$ devices with bandgaps, determined from composition, of 1.33, 1.48 and 1.74 eV, respectively. Possible causes for this discrepancy are compositional non-uniformity of the $\text{Cu}(\text{InAl})\text{Se}_2$ films or a change in the composition or phases present in the $\text{Cu}(\text{InAl})\text{Se}_2$ films resulting from the cell processing.

Table 2. J-V Parameters for $\text{Cu}(\text{InAl})\text{Se}_2$ Solar Cells.

| Al/(Al+In) | E_g (eV) | V_{oc} (V) | J_{sc} (mA/cm^2) | FF (%) | Eff. (%) |
|------------|------------|--------------|--------------------------------------|--------|----------|
| 0.00 | 1.0 | 0.438 | 33.6 | 66.7 | 9.8 |
| 0.26 | 1.33 | 0.517 | 30.6 | 69.7 | 11.0 |
| 0.36 | 1.48 | 0.630 | 25.5 | 65.8 | 10.6 |
| 0.53 | 1.74 | 0.711 | 18.2 | 54.0 | 7.0 |

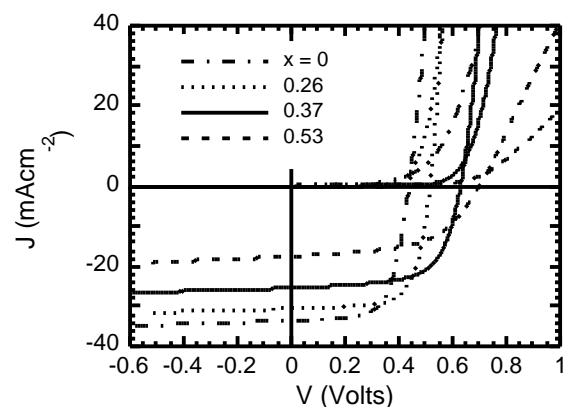


Fig. 8. Illuminated and dark J-V curves for $\text{Cu}(\text{InAl})\text{Se}_2$ devices.

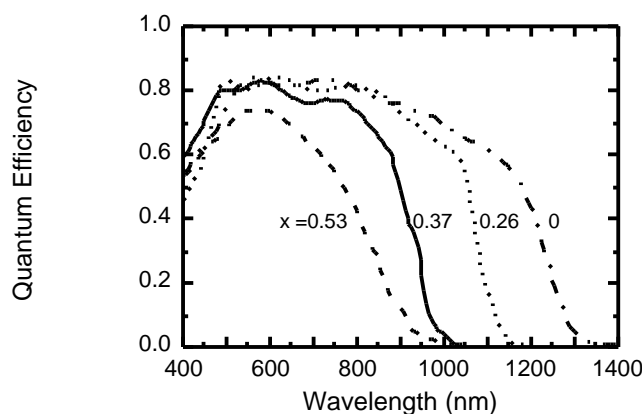


Fig. 9. Quantum efficiency curves for $\text{Cu}(\text{InAl})\text{Se}_2$ devices.

DISCUSSION AND CONCLUSIONS

Single phase $\text{Cu}(\text{InAl})\text{Se}_2$ films were deposited in a four-source elemental evaporation system. Optical and XRD measurements show that, by controlling the relative Al content, the band gap and lattice spacing of the $\text{Cu}(\text{InAl})\text{Se}_2$ films can be varied with predictable shifts in both parameters, in agreement with results obtained on $\text{Cu}(\text{InAl})\text{Se}_2$ crystals. In addition, the films have high optical transmission for sub-bandgap energy illumination.

$\text{Cu}(\text{InAl})\text{Se}_2$ devices have been demonstrated with the best performing device having 11 % efficiency after post fabrication air annealing. There is an apparent discrepancy between the QE long wavelength edge and the absorber layer bandgap with additional work needed to determine the cause.

This work has demonstrated that $\text{Cu}(\text{InAl})\text{Se}_2$ can be used to make thin film solar cells with variable band gap over a range appropriate for both high efficiency single junction cells and the top cell in a tandem device. However, higher efficiencies will be needed to make devices comparable to $\text{Cu}(\text{InGa})\text{Se}_2$ devices with similar bandgap. A possible approach to improving the device performance will be to utilize higher substrate temperatures but this will require improving the film adhesion. Another approach will be to evaluate modified deposition processes, for example by incorporating a Cu-rich growth stage during the film deposition.

ACKNOWLEDGEMENT

This work was supported, in part, by NIST under an Advanced Technology Program in collaboration with ITN Energy Systems and Global Solar Energy.

REFERENCES

- [1] W.N. Shafarman R. Klenk and B.E. McCandless, *J. Appl. Phys.* **79**, 7324 (1996).
- [2] V. Nadenau, D. Hariskos and H.W. Schock, *14th E.C. Photovoltaic Sol. Energy Conf.*, Barcelona, H. S. Stephens and Associates, Bedford, UK, (1997).
- [3] J. Klaer, J. Bruns, R. Henniger, K. Töpfer, R. Klenk, K. Ellmer and D. Bräunig, *Proc. 2nd. World Conf. On Photovoltaic Solar Energy Conversion*, Vienna, European Commission, 537 (1998).
- [4] S. Wei and A. Zunger, *J. Appl. Phys.* **78**, 3846 (1995).
- [5] W. Gebicki, M. Igalson, W. Zajac and R. Trykozko, *J. Phys. D: Appl. Phys.* **23**, 964 (1990).
- [6] C.A. Durante Rincón, M.T. Mora and M. León, *Inst. Phys. Conf. Ser.* No 152: Section A, 123 (1998).
- [7] I.V. Bodnar and I.N. Tsyrelchuk, *Journal of Materials Science Letters*, **13**, 762, (1994).
- [8] F. Itoh, O. Saitoh, M. Kita, H. Nagamore and H. Oike, *Solar Energy Materials and Solar Cells* **50**, 119 (1996).
- [9] Powder Diffraction Files, Ed. F. McClune (Joint Committee on Powder Diffraction Standards, Pennsylvania, 1997).

